NOT FOR PUBLICATION

INDC (JAP) 4 E
EANDC (J) 13 L
307

PROGRESS REPORT

(November 1968 to July 1969 inclusive)

August 1969

edited by

T. Momota

aided by

T. Fuketa and K. Okamoto

Japanese Nuclear Data Committee

Japan Atomic Energy Research Institute

Tokai Res... Establishment

Tokai-mura, Ibaraki-ken, Japan

NOT FOR PUBLICATION

INDC (JAP) 4 E
EANDC (J) 13 L

PROGRESS REPORT

(November 1968 to July 1969 inclusive)

August 1969

edited by

T. Momota

aided by

T. Fuketa and K. Okamoto

Japanese Nuclear Data Committee

Japan Atomic Energy Research Institute

Tokai Research Establishment

Tokai-mura, Ibaraki-ken, Japan

PREFACE

The reports, herein collected, present progress of those researches related to the nuclear data of interest to the development of the nuclear energy program. This edition covers a period of November 1, 1968 to July 31, 1969.

The informations herein contained are of a nature of "Private Communication." They should not be quoted without author's permission.

まえがき

この報告は原子力開発の基礎として必要な核データに関係のある研究で1968年11月1日から1969年7月末日までの期間にわが国で行なわれた仕事を対象として編集したものである。ここに記載された内容はCINDAに採録されるが，各個の報告は"private communication"として扱うべきもので，著者の許可なしには引用されない性質のものである。

なお，ここにいう核データとは，具体的には約20MeV以下の中性子の反応断面積（逆反応の断面積を含む）および核分裂に関する諸データを言う。1965年以来わが国が参加しているヨーロッパ・アメリカ核データ委員会（EANDC）では，その参加国に少なくとも1年に1度の割合で研究のprogress reportを出す事を義務づけており，本報告はこの委員会に提出される。

CONTENTS

CONTENTS (cont'd)

CONTENTS OF THE JAPANESE PROGRESS REPORT INDC(JAP)4E (=EANDC(J)13L), August 1969

ELEMENT S A	QUANTITY	TYPE	ENERGY MIN	MAX	DOCUMENTATION REF VOL PAGE DATE	LAB	COMMENTS
H 002	DIFF INELAST	EXPT-PROG	1.5 7		EANDC(J)13L,38 8/69	TIT	ARAI+.TOF,SEARCH FOR BREAK-UP IN FIG
LI 006	ELASTIC	EXPT-PROG	1.0 3	1.1 5	EANDC(J)13L, 6 8/69	HAR	ASAMI+.LINAC,S-WAVE SCAT,SIG IN FIG
BE 009	DIFF ELASTIC	EXPT-PROG	1.4 7		EANDC(J)13L,31 8/69	KYU	HYAKUTAKE+.TOF,10 TO 165DEG IN FIG
BE 009	DIFF INELAST	EXPT-PROG	1.4 7		EANDC(J)13L,31 8/69	KYU	HYAKUTAKE+.TOF,2.43MEV LVL IN FIG
B 010	DIFF ELASTIC	EXPT-PROG	1.4 7		EANDC(J)13L,29 8/69	KYU	HYAKUTAKE+.TOF,COMPLEX N-GROUP,FIG
B 010	DIFF INELAST	EXPT-PROG	1.4 7		EANDC(J)13L,29 8/69	KYU	HYAKUTAKE+.TOF,5 COMPLEX N-GROUP
B 011	DIFF ELASTIC	EXPT-PROG	1.4 7		EANDC(J)13L,29 8/69	KYU	HYAKUTAKE+.TOF 10 TO 160DEG IN FIG
B 011	DIFF INELAST	EXPT-PROG	1.4 7		EANDC(J)13L,29 8/69	KYU	HYAKUTAKE+.TOF 4 COMPLEX N-GROUPS
C	TOTAL XSECT	REVW-PROG	0	2.0 6	EANDC(J)13L,20 8/69	JAE	NISHIMURA+.LEAST SQUARES FIT,TBP
C 012	DIFF ELASTIC	EXPT-PROG	1.4 7		EANDC(J)13L,36 8/69	JAP	AZUMA+.VDG,TOF.
C 012	DIFF INELAST	EXPT-PROG	1.4 7		EANDC(J)13L,36 8/69	JAP	AZUMA+.VDG,TOF.SIG AT 35DEG GIVN
N	DIFF INELAST	EXPT-PROG	1.4 7		EANDC(J)13L,33 8/69	KYU	MATOBA+.TBD BY IMPROVED TOF
O 016	DIFF ELASTIC	EXPT-PROG	1.4 7		EANDC(J)13L,36 8/69	JAP	AZUMA+.VDG,TOF.
O 016	DIFF INELAST	EXPT-PROG	1.4 7		EANDC(J)13L,36 8/69	JAP	AZUMA+.VDG,TOF.SIG AT 35DEG GIVN
AL 027	DIFF ELASTIC	THEO-PROG	4.8 6	8.0 6	EANDC(J)13L,12 8/69	JAE	TSUKADA+.OPTMDL CALC,FIG+TABLE
AL 027	DIFF ELASTIC	EXPT-PROG	1.4 7		EANDC(J)13L,36 8/69	JAP	AZUMA+.VDG,TOF
AL 027	DIFF INELAST	THEO-PROG	4.8 6	8.0 6	EANDC(J)13L,12 8/69	JAE	TSUKADA+.H-F CAL FOR 1ST+2ND LVL,FIG
AL 027	DIFF INELAST	EXPT-PROG	1.4 7		EANDC(J)13L,36 8/69	JAP	AZUMA+.VDG,TOF.SIG AT 35DEG GIVN
SI	DIFF ELASTIC	THEO-PROG	4.8 6	8.0 6	EANDC(J)13L,12 8/69	JAE	TSUKADA+.OPTMDL CALC,FIG+TABLE
SI 028	DIFF INELAST	THEO-PROG	4.8 6	8.0 6	EANDC(J)13L,12 8/69	JAE	TSUKADA+.H-F CALC FOR 1ST LVL,FIG
SI 028	N,PROTON	EXPT-PROG	PILE		EANDC(J)13L,23 8/69	KYO	KIMURA+.THRESHOLD REACT.AV SIG GIVN
SI 029	N,PROTON	EXPT-PROG	PILE		EANDC(J)13L,23 8/69	KYO	KIMURA+.THRESHOLD REACT.AV SIG GIVN
SI 030	N,ALPHA	EXPT-PROG	PILE		EANDC(J)13L,23 8/69	KYO	KIMURA+.THRESHOLD REACT.AV SIG GIVN
S	DIFF ELASTIC	THEO-PROG	4.5 6	8.0 6	EANDC(J)13L,12 8/69	JAE	TSUKADA+.OPTMDL CALC,NDG
S 032	DIFF INELAST	THEO-PROG	4.5 6	8.0 6	EANDC(J)13L,12 8/69	JAE	TSUKADA+.H-F CALC,NDG
TI 046	N,PROTON	EXPT-PROG	PILE		EANDC(J)13L,23 8/69	KYO	KIMURA+.THRESHOLD REACT.AV SIG GIVN
TI 047	N,PROTON	EXPT-PROG	PILE		EANDC(J)13L,23 8/69	KYO	KIMURA+.THRESHOLD REACT.AV SIG GIVN
TI 048	N,PROTON	EXPT-PROG	PILE		EANDC(J)13L,23 8/69	KYO	KIMURA+.THRESHOLD REACT.AV SIG GIVN
CR	N,GAMMA	THEO-PROG	3	6	EANDC(J)13L,21 8/69	JAE	NISHIMURA+.COMPUTER CALC,NDG
FE	DIFF ELASTIC	EXPT-PROG	1.4 6	3.3 6	EANDC(J)13L,12 8/69	JAE	TSUKADA+.PUBLISHED IN NP A125 P641
FE	DIFF ELASTIC	EXPT-PROG	1.4 6	2.2 6	EANDC(J)13L,16 8/69	JAE	TOMITA.MEASUREMENT COMPLETED NDG
FE	DIFF INELAST	EXPT-PROG	1.4 6	3.3 6	EANDC(J)13L,12 8/69	JAE	TSUKADA+.PUBLISHED IN NP A125 P641
FE	N,GAMMA	THEO-PROG	3	6	EANDC(J)13L,21 8/69	JAE	NISHIMURA+.COMPUTER CALC,NDG
FE 056	DIFF INELAST	EXPT-PROG	1.4 6	2.2 6	EANDC(J)13L,16 8/69	JAE	TOMITA.MEASUREMENT COMPLETED NDG

ELEMENT S A	QUANTITY	TYPE	ENERGY MIN	MAX	DOCUMENTATION REF VOL PAGE	DATE	LAB	COMMENTS
CO 059	TOTAL XSECT	EXPT-PROG	1.1 6	1.4 6	EANDC(J)13L,41	8/69	ISS	NAGAMINE+.SPIN-SPIN INTERACT,POLRZ
CO 059	TOTAL XSECT	EXPT-PROG	7.9 6		EANDC(J)13L,42	8/69	ISS	KOBAYASHI+.SPIN-SPIN INT.PUB IN PTP
NI	DIFF ELASTIC	EXPT-PROG	2.0 6	3.3 6	EANDC(J)13L,12	8/69	JAE	TSUKADA+.PUBLISHED IN NP A125 P641
NI	DIFF INELAST	EXPT-PROG	2.0 6	3.3 6	EANDC(J)13L,12	8/69	JAE	TSUKADA+.PUBLISHED IN NP A125 P641
NI	N,GAMMA	THEO-PROG	3	6	EANDC(J)13L,21	8/69	JAE	NISHIMURA+.COMPUTER CALC,NDG
CU	DIFF ELASTIC	THEO-PROG	1.7 6	2.2 6	EANDC(J)13L,12	8/69	JAE	TSUKADA+.OPTMDL+MOLDAUER
CU	DIFF INELAST	THEO-PROG	1.7 6	2.2 6	EANDC(J)13L,12	8/69	JAE	TSUKADA+.H-F+MOLDAUER,FIG+TABLE
ZN	DIFF ELASTIC	THEO-PROG	1.7 6	8.0 6	EANDC(J)13L,12	8/69	JAE	TSUKADA+.OPTMDL+MOLDAUER,FIG+TABLE
ZN	DIFF INELAST	THEO-PROG	1.7 6	8.0 6	EANDC(J)13L,12	8/69	JAE	TSUKADA+.H-F+MOLDAUER,FIG+TABLE
ZN 064	N,PROTON	EXPT-PROG	PILE		EANDC(J)13L,23	8/69	KYO	KIMURA+.THRESHOLD REACT AV SIG GIVN
MO	N,GAMMA	THEO-PROG	3	6	EANDC(J)13L,21	8/69	JAE	NISHIMURA+.COMPUTER CALC,NDG
CS 133	INELAST GAMMA	EXPT-PROG	5.0 5	1.0 6	EANDC(J)13L,15	8/69	JAE	KIKUCHI+.NEW 4 GAMS.ANGDIST
LA	TOTAL XSECT	EXPT-PROG	1.0 4	2.4 5	EANDC(J)13L,16	8/69	JAE	NISHIMURA+.MEASUREMENT COMPLETED
PR 141	TOTAL XSECT	EXPT-PROG	1.0 4	2.4 5	EANDC(J)13L,16	8/69	JAE	NISHIMURA+.MEASUREMENT COMPLETED
ND 143	N,ALPHA	EXPT-PROG	2.5-2		EANDC(J)13L, 3	8/69	JAE	OKAMOTO.SIGS TO CE140 LVLS IN TABLE
ND 145	N,ALPHA	EXPT-PROG	2.5-2		EANDC(J)13L, 3	8/69	JAE	OKAMOTO.SIGS TO CE142 LVLS IN TABLE
SM 147	N,ALPHA	EXPT-PROG	2.5-2		EANDC(J)13L, 3	8/69	JAE	OKAMOTO.SIGS TO ND144 LVLS IN TABLE
SM 149	TOTAL XSECT	EXPT-PROG	2.5-2		EANDC(J)13L, 1	8/69	JAE	ASAMI+.SIG=37000 PM 1600 B
SM 149	RESON PARAMS	EXPT-PROG	9.9-2		EANDC(J)13L, 1	8/69	JAE	ASAMI+.WT=59.5 PM 0.8 MILLI-EV
SM 149	N,ALPHA	EXPT-PROG	2.5-2		EANDC(J)13L, 3	8/69	JAE	OKAMOTO.SIGS TO ND146 LVLS IN TABLE
GD 155	TOTAL XSECT	EXPT-PROG	9.0-4	3.0-1	EANDC(J)13L, 2	8/69	JAE	OHNO+.SIG IN FIG.RES-PARAMETER TBP
GD 157	TOTAL XSECT	EXPT-PROG	9.0-4	3.0-1	EANDC(J)13L, 2	8/69	JAE	OHNO+.SIG IN FIG.RES-PARAMETER TBP
W	DIFF ELASTIC	EXPT-PROG	1.4 6	2.0 6	EANDC(J)13L,12	8/69	JAE	TSUKADA+.PUBLISHED IN NP A125 P641
W	DIFF INELAST	EXPT-PROG	1.4 6	2.0 6	EANDC(J)13L,12	8/69	JAE	TSUKADA+.PUBLISHED IN NP A125 P641
RE 185	RESON PARAMS	EXPT-PROG	0	1.2 2	EANDC(J)13L, 5	8/69	JAE	IDENO+.AGREE WITH FRIESENHAHN+.TBP
RE 187	RESON PARAMS	EXPT-PROG	0	1.2 2	EANDC(J)13L, 5	8/69	JAE	IDENO+.AGREE WITH FRIESENHAHN+.TBP
PB 204	TOT INELASTC	EXPT-PROG	PILE		EANDC(J)13L,23	8/69	KYO	KIMURA+.THRESHOLD REACT.AV SIG GIVN
PB 204	N2N XSECTION	EXPT-PROG	PILE		EANDC(J)13L,23	8/69	KYO	KIMURA+.THRESHOLD REACT.AV SIG GIVN
PB 208	DIFF ELASTIC	EXPT-PROG	1.4 7		EANDC(J)13L,36	8/69	JAP	AZUMA+.VDG,TOF
PB 208	DIFF INELAST	EXPT-PROG	1.4 7		EANDC(J)13L,36	8/69	JAP	AZUMA+.VDG,TOF SIG AT 35DEG GIVN
U 238	DIFF INELAST	THEO-PROG	TR	1.5 7	EANDC(J)13L,20	8/69	JAE	IGARASI+.H-F AND EVAPORATION,NDG
MANY	SCATTERING	COMP-PROG	2.0 5	9.0 6	EANDC(J)13L,22	8/69	JAE	IGARASI+.TRANSMIS-COEF FOR A=20 TO 79
MANY	FISSION	THEO-PROG	SPON		EANDC(J)13L,19	8/69	JAE	E.TAKEKOSHI.SYSTEMATICS ON HALF-LIFE
MANY	LVL DEN LAW	EXPT-PROG	2.0 6	7.5 6	EANDC(J)13L,10	8/69	JAE	MARUYAMA+.PUBLISHED IN NP A131 P145

I. Japan Atomic Energy Research Institute

A. Neutron Experiments - Reactor

I-A-1. The Parameters of the 0.099-eV Neutron Resonance in Sm-149

T. Asami, K. Okamoto, K. Ideno and Y. Ohno

A full paper on this subject was published in the Journal of the Physical Society of Japan 26 (1969) 225 with an abstract as follows :

Measurements of the 0.099-eV resonance in Sm-149 have been made with a crystal spectrometer and a neutron velocity selector in the energy range from 0.0006 to 1 eV. Samples highly enriched to 97.42 % in Sm-149 were used. The observed neutron transmissions were analysed by a shape method using a Breit-Wigner single level formula. The resonance parameters obtained from the analysis are ; $E_0 = 0.0989 \pm 0.0008$ eV, $\Gamma = 59.5 \pm 0.8$ meV, and $\Gamma_n^0 = 1.71 \pm 0.03$ meV, assuming the statistical weight factor is 9/16. The 2200 m/sec value of the total cross section is 37,000 ± 1,600 barns.

The final values of the parameters are the same as the values which had been reported in the progress report, EANDC (J) 8 "L", p. 1, (1968).

I-A-2. The Parameters of the Low-Lying Neutron Resonances in Gd-155 and Gd-157

Y. Ohno, T. Asami, K. Okamoto, K. Ideno and S. Ohtomo

The measurements of the total cross-section for ^{155}Gd and ^{157}Gd were outlined in the previous report, EANDC (J) 10 "L", p. 2, Nov. 1968.

The cross section curves are shown in the Figure. These data were analysed to obtain the parameters of the low-lying neutron resonances. The values of the parameter (E_o, Γ_n^0, Γ) are in agreement with the values of MØller et al.[1] for both Gd isotopes. The details will be published in near future.

Reference :

1) H.B. MØller, F.G. Shore and V.L. Sailor, Nucl. Sci. and Eng., 8 (1960) 183.

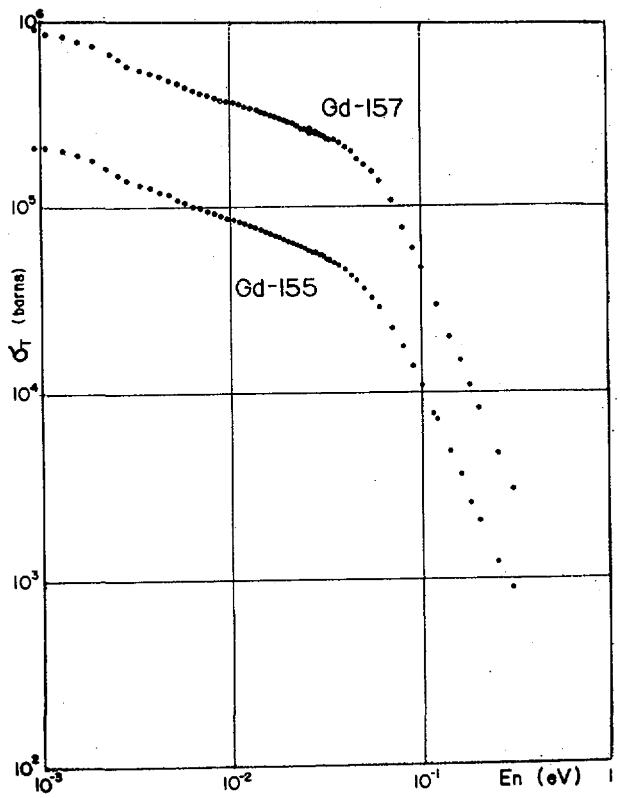

I-A-3. The Thermal-Neutron Induced (n, α) Reactions in Rare-Earth Elements

K. Okamoto

The (n, α) reaction was investigated on ^{147}Sm, ^{149}Sm, ^{143}Nd and ^{145}Nd for the thermal neutrons, and the effective cross sections were obtained.

The reaction cross sections at the neutron energy of 0.0253 eV ("2200 m/sec" values) were deduced from the observed neutron spectrum of JRR-2. The preliminary results of ^{149}Sm, and ^{143}Nd (n, α) reaction were represented in EANDC (J) 8 "L", p. 1, 1968. The final results are summarized in the table. A full paper on this experiment will be published as "The (n, α) Reaction on Samarium and Neodymium Isotopes induced by Thermal Neutrons".

Table Results on the (n_{th}, α) Reaction

Target Nucleus	E_α (MeV)	Residual Nucleus	$\hat{\sigma}_\alpha$ (mb)	$\sigma_{0\alpha}$ (mb)	Reduced alpha Width δ^2 (eV)
^{149}Sm	9.19	^{146}Nd gnd 0^+	8.2 ± 0.8	5.0 ± 0.5	3.0
	8.74	1st 2^+	35.4 ± 5.7	23.5 ± 3.7 {19.4 (from 4^-), 4.1 (from 3^-)}	6.9
	8.18	2nd 4^+	~ 1.6 ± 0.8	~1.1 ± 0.6 {1.0 (from 4^-), 0.1 (from 3^-)}	1.2
	8.02	3rd 3^- etc	~ 1.8	~1.2 {1.0 (from 4^-), 0.2 (from 3^-)}	4.0
^{143}Nd	9.44	^{140}Ce gnd 0^+	25.2 ± 3.0	15.5 ± 1.6	11.4
	7.89	1st 2^+	$\lesssim$ 0.3	$\lesssim$ 0.2	<16.6
	7.59	2nd 0^+	$\lesssim$ 0.3	$\lesssim$ 0.2	.....
^{147}Sm	9.85	^{144}Nd gnd 0^+	0.29 ± 0.06	0.18 ± 0.04	0.3
	9.17	1st 2^+	0.86 ± 0.17	0.53 ± 0.10	2.4
^{145}Nd	8.57	^{142}Ce gnd 0^+	~ 0.2	$\lesssim$ 0.1	< 7.0
	7.94	1st 2^+	~ 0.2	$\lesssim$ 0.1	< 27

$\hat{\sigma}_\alpha$ is the effective cross section for the neutron spectrum used, $\sigma_{0\alpha}$ is the cross section at the neutron energy of 0.0253 eV.

I-A-4. Nuclear Resonant Scattering of 6734-keV Lead Capture Gamma-Ray from ^{120}Sn

N. Shikazono and Y. Kawarasaki

The nuclear resonant scattering of the 6734-keV lead capture gamma-ray was studied by means of a 20 cc Ge(Li) detector.

About 5-kg natural lead which served as the gamma-ray source was inserted into an experimental tube of the 10-MW research reactor, JRR-3. Natural tin was used as the scatterer. A new electronic system which rejects the slow-risetime pulses and also pile-up pulses was used in order to obtain a better resolution and a better signal-to-noise ratio.

In the spectrum of the scattered gamma-rays, two peaks at 6734 keV and 5558 keV were observed. The 6734-keV gamma-ray is an elastically scattered one and the 5558-keV gamma-ray corresponds to an inelastic transition from the 6734-keV resonant level to the 1176-keV level.

The measurement of the angular distribution of the 6734-keV gamma-ray was performed. The results indicate that the spin sequence should be 0-1-0, viz., the isotope responsible for the resonant scattering should be even-even. The energy of the level fed by the 5558-keV inelastic transition is 1176 keV in agreement with the energy of the first excited state of ^{120}Sn. Consequently, it would be concluded that the resonant isotope is ^{120}Sn.

B. Neutron Experiments - Linac

I-B-1. Neutron-Resonance Parameters for Re

K. Ideno, T. Asami, Y. Nakajima, M. Ohkubo and T. Fuketa

The neutron transmission measurements for Re were outlined in the previous progress report (EANDC (J) 10 "L", p. 5, Nov. 1968). The analyses on these data have been performed with both the shape and the area method. The parameters of about sixty resonances of Re^{185} and Re^{187} are obtained below 120 eV of the neutron energy. Most of the parameters are in good agreement with those obtained by Friesenhahn et al.[1] rather than the recommended values in the BNL-325.[2] The details will be published in near future.

References :

1) S.J. Friesenhahn, D.A. Gibbs, E. Haddad, F.H. Fröhner and W.M. Lopez, J. Nucl. Energ., 22 (1968) 191.

2) BNL-325 2nd ed. Suppl. No. 2, Vol. IIC (1966).

I-B-2. Low Energy Neutron Scattering Cross-section of ^{6}Li

A. Asami* and M.C. Moxon**

The neutron scattering cross-section of ^{6}Li has been measured in the energy region between 1 keV and 110 keV with a scattering detector on a 50 m flight path of the Harwell Electron Linac neutron time of flight spectrometer.

The detector and the experimental arrangement are the same as those used for the ^{10}B scattering cross-section measurements described in ref. 1). Briefly, the detector consists of eight ^{6}Li-glass scintillators and the measurements were made at four angles to the incident neutrons ; 39^{o}, 65^{o}, 120^{o} and 144^{o}, respectively.

The ^{6}Li sample is 1.97" in diameter, and has a thickness of 5.88×10^{-2} atoms/b (93.7 % ^{6}Li, 5.2 % ^{7}Li, and 1.1 % others). The sample is canned with a thin aluminium plate with a thickness of 1.47×10^{-3} atoms/b, which is sealed with Araldite. The measurements were made relative to a carbon sample, which is 1.37" in diameter with a thickness of 2.06×10^{-3} atoms/b. The incident neutrons were collimated to 0.9" in diameter.

The data were analysed in a similar way as in ref. 1). In the analysis corrections for the effect of the following were made ; (1) self absorption in the sample, (2) the sample impurities, (3) the sample can, (4) the energy dependence of the detector efficiency, (5) the size of the detector, and (6) the multiple scattering. The effect of self absorption is fairly large in the low energy region, e.g., relative corrections at 1, 10 and 70 keV at 65^{o} are 1.52, 1.09 and 1.00, respectively. The order of magnitudes of the

---

* The measurements were carried out when A. Asami was at AERE, Harwell, U.K.

** AERE, Harwell, Didcot, Berks. U.K.

other corrections averaged over angle are shown in Table 1. Above 40 keV one more correction is required. A scattered neutron passes through an aluminium vacuum tube with a thickness of 0.064" before reaching the detector. Because of an appreciable energy difference between the neutrons scattered from the ^{6}Li and the carbon sample, attenuation of the neutrons due to the tube is different between the two cases. The correction for this effect is in progress.

The differential scattering cross-section thus obtained showed no significant angular dependence below 10 keV, so that the total scattering cross-section was obtained assuming pure s-wave scattering. The results are shown in Fig. 1. The cross section near 2.8 keV was not measured because of the presence of a resonance in sodium permanently left in the flight path to normalize the backgrounds. The errors are a combination of uncertainties arising from counting statistics, background, and multiple scattering (± 30 % are assumed). The second is the most significant (about 3/2 of either of the others) and the other two contribute equally.

From Fig. 1 the cross-section appears to be constant between 10 keV and 4 keV, but becomes slightly lower below 2 keV. This decrease is most probably due to inaccuracy in the applied corrections. The averaged cross-section over energy between 0.91 and 10.3 keV is 0.801 ± 0.036 b. In the low energy region a constant deviation $\Delta\sigma$ of the ^{6}Li (n, α) cross-section from 1/v law[2)] is estimated to be -0.03 ± 0.01 b by Bergman and Shapilo.[3)] Diment and Uttley[4)] obtained the least square fit to their total cross-section data of ^{6}Li below 5 keV with $(149.5 \pm 0.3)/\sqrt{E}$ (in eV) + (0.696 ± 0.010). With this expression and the value of the constant scattering cross-section obtained in the present work $\Delta\sigma$ is -0.105 ± 0.037 b.

References :

1) A. Asami and M.C. Moxon, AERE-R 5980 (1969).

2) F.L. Shapiro, JETP 34 (1958) 1648 ; Soviet Physics JETP 7 (1958) 1132.

3) A.A. Bergman and F.L. Shapiro, JETP 40 (1961) 1270 ; Soviet Physics JETP 13 (1961) 895.

4) K.M. Diment and C.A. Uttley, Nuclear Physics Division Report AERE PR/NP 14.

Table 1. Order of Magnitude of Corrections (%)

Energy (keV)	1	10	70
Impurities	-2	0	2
Sample Can	-10	-7	-8
Detector Efficiency	-8	-8	-6
Detector Size	1	0	0
Multiple Scattering	11	10	8

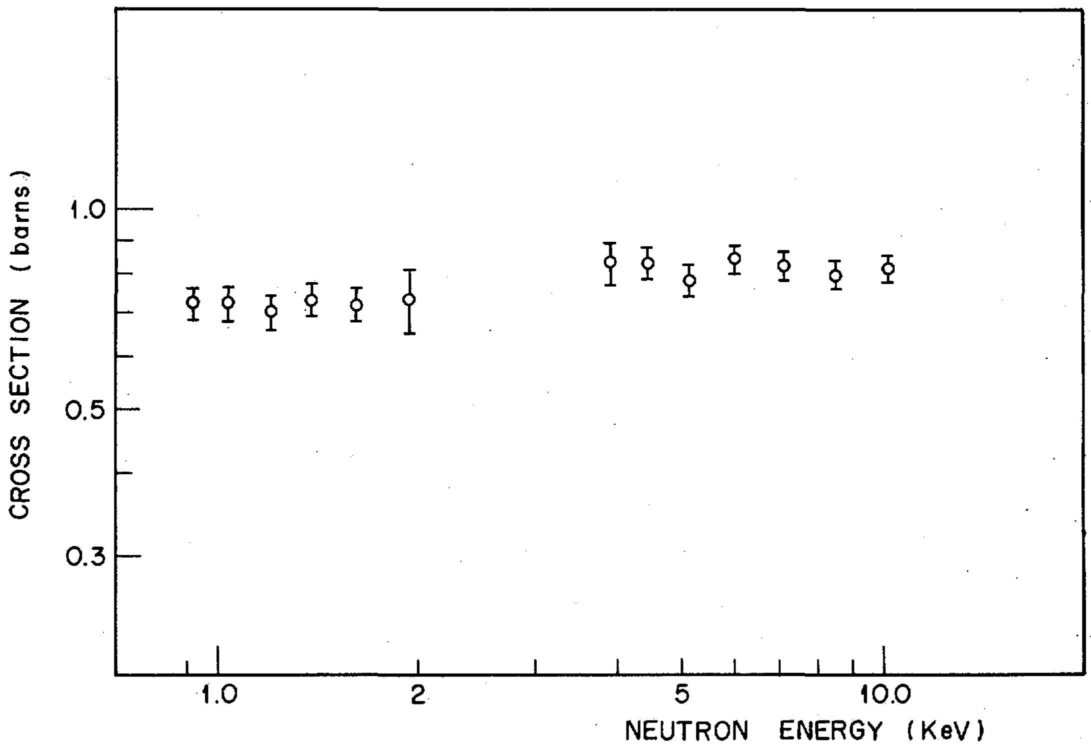

Fig. 1 TOTAL SCATTERING CROSS-SECTION OF ^{6}Li

I-B-3. An Effect of Scattered Neutrons from Photomultipliers on the Neutron Spectrum Measured by ^{6}Li Glass Scintillators

M. Ohkubo

A paper on this subject was published in Nuclear Instruments and Methods 65 (1968) 113 with an abstract as follows :

The neutron spectrum measured by ^{6}Li glass scintillators has been found to have an enhancement peak at E_n = 2.87 keV, due to resonance scattering from ^{23}Na contained in the glass of photomultipliers.

C. Neutron Experiments - Van de Graaff Accelerator

I-C-1. Energy Dependence of the Nuclear Level Density

M. Maruyama, K. Tsukada, S. Tanaka and Y. Tomita

A full paper of this work, which was outlined in the previous report (EANDC (J) 10 "L" p. 12), was published in Nuclear Physics A131 (1969) 145 ~ 168.

I-C-2. Direct Measurement of Nuclear Reaction Times by the Use of the Blocking Effect in Single Crystals

M. Maruyama, K. Tsukada, K. Ozawa, F. Fujimoto,* K. Komaki,* M. Mannami,** and T. Sakurai**

A new method to measure reaction times by the use of the blocking effect of energetic charged particles in single crystals was applied to the $^{28}Si(p,p')^{28}Si$ (1st excited state, 1.78 MeV, 2^+), $^{70}Ge(p,p')^{70}Ge$ (1st excited state, 1.04 MeV, 2^+) and $^{72}Ge(p,p')^{72}Ge$ (2nd excited state, 0.835 MeV, 2^+) reactions. The angular distributions of protons scattered from thin single crystals at scattering angles of 88° to 92° were measured at incident energies of 1.79, 3.61, 4.02, 4.21, 4.56, 5.45 and 5.86 MeV for silicon and of 3.36, 3.77, 4.36, 4.84, 5.42 and 5.91 MeV for germanium. The center-of-mass motion was normal to the (111) plane and the blocking dip by the (111) plane was observed at about 90° to the incident beam. Two-parameter

---

* Institute of Physics, College of General Education, University of Tokyo, Tokyo.

** Department of Physics, Kyoto University, Kyoto.

pulse-height analysis of both the energies and the directions of the scattered protons was performed by the use of a position-sensitive surface barrier detector.

Since the dominant process of the elastic scattering in the present experiment is the Rutherford scattering which has small impact parameters (10^{-4} Å) and an extremely short reaction time, its blocking pattern can be used as the standard pattern without any reaction time effect. The blocking dip areas observed for the $^{70}Ge(p,p')^{70}Ge$ and $^{72}Ge(p,p')^{72}Ge$ reactions showed a clear reduction from the elastic values. Reaction times estimated from the reduction are shown in table 1. No reduction was observed for $^{28}Si(p,p')^{28}Si$ (1st excited state, 1.78 MeV, 2^+) at any energy.

A short report of this work was published in Physics Letters 29B (1969) 414 ~ 416.

Table 1. Reaction times τ for the inelastic scattering of protons by germanium

Incident energy E_P (MeV)	τ (s)	
	$^{70}Ge(p,p')^{70}Ge$ 1.04 MeV, 2^+	$^{72}Ge(p,p')^{72}Ge$ 0.835 MeV, 2^+
4.84	$(3.4 \pm 2.1) \times 10^{-17}$	$(4.1 \pm 1.8) \times 10^{-17}$
5.42	$(3.1 \pm 1.3) \times 10^{-17}$	$(2.3 \pm 0.9) \times 10^{-17}$
	$(3.7 \pm 1.8) \times 10^{-17}$	$(2.3 \pm 1.0) \times 10^{-17}$
5.91	$(2.2 \pm 1.3) \times 10^{-17}$	$< 0.5 \times 10^{-17}$

I-C-3. Elastic and Inelastic Scattering of Fast Neutrons from Iron, Nickel and Tungsten

K. Tsukada, S. Tanaka, Y. Tomita and M. Maruyama

A full paper of this work, which was outlined in the previous report (EANDC (J) 8 "L" p. 17), was published in Nuclear Physics A125 (1969) 641 ~ 653.

I-C-4. Analysis of Angular Distributions of Fast Neutrons Scattered by Al, Si, S, Cu and Zn

K. Tsukada, Y. Tomita, S. Tanaka and M. Maruyama

Angular distributions[1)] of fast neutrons scattered by Al, Si, S, Cu and Zn have been analyzed by the use of the optical model and the statistical model at energies of 4.8, 6.0, 7.0 and 8.0 MeV for Al, Si, S and Zn (4.5 MeV in stead of 4.8 MeV for S and Zn) (case 1), and at energies of 1.71 and 2.24 MeV for Cu and Zn (case 2). In the case 1 the Hauser-Feshbach formula is used for the statistical-model calculation, and in the case 2 the Moldauer theory is used in addition to the Hauser-Feshbach formula. In the Moldauer calculation, the resonance interference contribution is taken into account with explicit dependence of the parameter Q_c on the partial strength function,[2)] and with the value of $Q_c = 0$. Some of the results are shown in Figs. 1 ~ 3 and Table.

References :

1) S. Tanaka et al., EANDC (J) 10 "L" (1968) p. 8 and p. 9.

2) Y. Tomita, EANDC (J) 10 "L" (1968) p. 11.

Table 1. Optical-model parameters

Element	Al	Si	Zn	Zn	Zn
Type	H - F	H - F	H - F	Q_{max}	Q = 0
E_n (MeV)	4.81	4.81	1.71	1.71	1.71
V (MeV)	51.1	63.7	56.5	53.7	52.1
W (MeV)	8.60	5.87	2.70	12.1	9.56
V_{so} (MeV)	10.0	10.0	10.0	10.0	0.653
r_o (fm)	1.20	1.20	1.21	1.20	1.21
r_s (fm)	1.20	1.20	1.21	1.24	1.26
a (fm)	0.663	0.725	0.213	0.624	0.441
b (fm)	0.505	0.513	0.819	0.410	0.444
χ^2	2.0	35	0.80	1.7	15
$\sigma_{t,cal}$(b)	2.29	3.41	3.01	3.14	3.10
$\sigma_{t,obs}$(b)	2.25 ± 0.15	2.80 ± 0.20	3.2 ± 0.2	3.2 ± 0.2	3.2 ± 0.2

NOTE

H-F : the Hauser-Feshbach theory is used in the calculation of the compound process.

Q_{max} : the Moldauer theory is used with explicit dependence of the parameter Q on the partial strength function. (See Ref. 4).

Q=0 : the Moldauer theory is used, where the resonance interference contribution is neglected.

The optical-model potential is of a form,

$$V(r) = -Vf(r) - i\,Wg(r) - V_{so}\,\frac{1}{r}h(r)\lambda\!\!\!{}^{-2}\,\pi\,\vec{\ell}\cdot\vec{\sigma},$$

$$f(r) = \left[1+\exp\{(r-R_0)/a\}\right]^{-1},$$

$$g(r) = 4\exp\{(r-R_s)/b\}\left[1+\exp\{(r-R_s)/b\}\right]^{-2},$$

$$h(r) = \frac{1}{a}\exp\{(r-R_0)/a\}\left[1+\exp\{(r-R_0)/a\}\right]^{-2},$$

$$R_0 = r_o A^{1/3}, \quad R_s = rA^{1/3}.$$

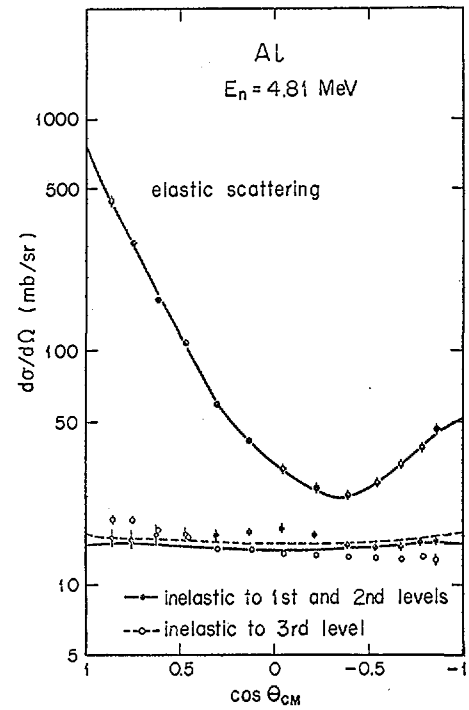

Fig. 1

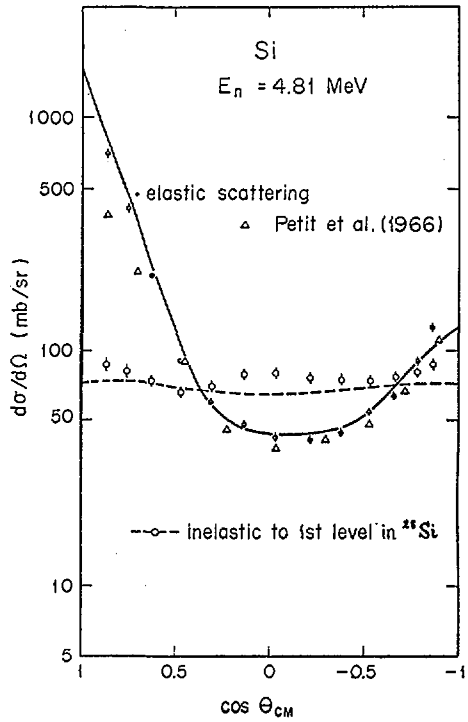

Fig. 2

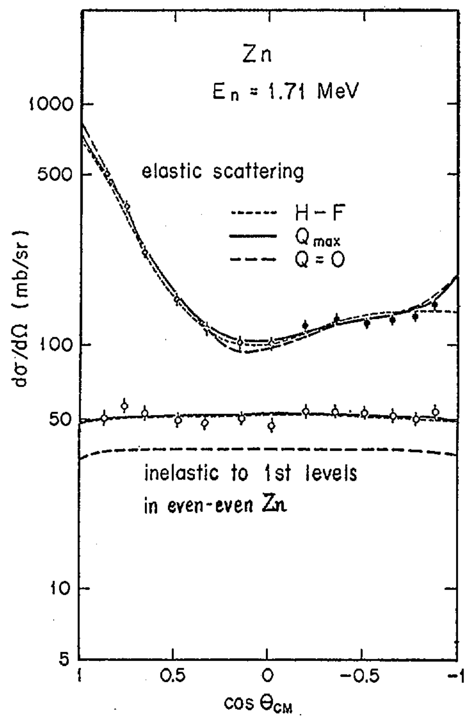

Fig. 3

I-C-5. Excited Levels of ^{133}Cs by Neutron Inelastic Scattering

S. Kikuchi, Y. Yamanouti, M. Maruyama and K. Nishimura

In order to study the excited levels of ^{133}Cs, the ^{133}Cs (n, n'γ) reaction was utilized. Low lying levels of ^{133}Cs have been investigated by several authors by means of the beta decay of ^{133}Ba or ^{133}Xe. The energies and spin-parities of the first four levels are well established, namely, 81.0 ($5/2^+$), 160.5 ($5/2^+$), 382 ($3/2^+$) and 437 ($1/2^+$) keV.[1)] However, higher levels than these four levels cannot be populated by the beta decay of ^{133}Ba or ^{133}Xe and none has been found so far.

A 17 cc co-axial type Ge(Li) detector, energy resolution of which was about 7 keV at 1 MeV, was used to detect the gamma rays, and a pulsed-beam time-of-flight system was also used to suppress backgrounds due to the interactions of neutrons with the detector.

Four gamma-rays of energies of 626, 633, 706 and 769 keV were observed in addition to the gamma-rays previously known. Excitation functions in an energy range of 0.5 $\sim$ 1.0 MeV of neutrons in steps of about 10 keV, and angular distributions at 0.960 MeV and 0.828 MeV from 30° to 120° were measured for those gamma-rays.

The energies of levels associated with the individual gamma-rays are derived from the thresholds of the excitation curves, and the informations about spin-parities of the levels from the angular distributions.

Detailed analyses of the data are now in progress.

Reference :

1) C.M. Lederer et al., Table of Isotopes, Sixth Edition, John Willey and Sons, INC.

I-C-6. Elastic and Inelastic Scattering of Neutrons in 20 MeV Region

Y. Yamanouti, S. Kikuchi, K. Tsukada and K. Nishimura

Preliminary experiments to get informations on neutron background and shielding have been carried out by a time-of-flight spectrometer including n-γ discrimination. The analysis of the results is now in progress.

I-C-7. Scattering of 1.5 to 2.0 MeV Neutrons by Iron

Y. Tomita, K. Tsukada and M. Maruyama

Measurement of the differential cross sections for elastic and inelastic scattering of neutrons from iron has been completed, at neutron energies of 1.44 to 2.15 MeV in 40 keV-steps, and the analysis of the results is now in progress.

I-C-8. Neutron Total Cross Section Measurements of La and Pr

K. Nishimura, Y. Yamanouti and S. Kikuchi

The measurements of the total neutron cross section of natural lanthanum and praseodymium have been completed in the energy range from 10 to 240 keV. Analyses of the data are now in progress by using an optical-model program, ELIESE-2, to obtain s- and p- wave strength functions of these nuclides.

I-C-9. STAX2 - A Computer Program for Calculating Neutron Elastic and Inelastic Scattering Cross Sections by means of the Optical Model and Moldauer's Theory

Y. Tomita

STAX 2 is a computer program for calculating neutron elastic and inelastic scattering cross sections by using the optical model and Moldauer's theory of the statistical model, and can search for the potential parameters which can reproduce experimental cross sections. Search is made on all potential parameters with respect to any combination of the following cross sections :

1) total cross section,
2) elastic scattering cross section (integral or differential),
3) inelastic scattering cross section for the first excited level (integral or differential).

Although there exist many optical model programs, none of them does not use Moldauer's theory for calculations of the compound nuclear process. The program NEARREX, often used to compute reaction cross sections by using Moldauer's Theory, does not include an optical model routine and can not calculate angular distributions. These are the resons why the present program has been developed.

In this program some improvements are made in the treatment of the resonance interference by taking into consideration the dependence of the parameter $Q^{J\pi}$ on $\langle \Gamma/D \rangle$.

A full report will be published soon.

D. Others

I-D-1. A Study of the Decay Scheme of ^{134}I

E. Takekoshi, H. Umezawa and T. Suzuki

A paper on this subject is to be published in Nuclear Physics.

Abstract: The decay properties of ^{134}I obtained from fission products have been investigated with NaI(Tl) and Ge(Li) detectors. Energies (and relative intensities) of the gamma-rays, determined from the Ge(Li) detector and NaI(Tl)-Ge(Li) coincidence studies, are 136(5.0), 236(weak), 405(8.4), 433(4.2), 488(weak), 514(4.1), 541(9.8), 596(11.6), 622(10.3), 633(3.1), 644(weak), 677(7.7), 733(weak), 768(3.9), 848(100.0), 859(6.1), 873(weak), 885(69.1), 905(weak), 923(weak), 948(6.4), 976(5.4), 1041(3.2), 1073(17.1), 1103(2.3), 1138(11.8), 1458(4.3), 1615(4.7), 1743(3.0) and 1810(6.2) keV. Gamma-ray coincidence spectra with the Ge(Li) detector were obtained with six gates ; the lower half, the higher half, and the total of gamma-ray peaks at 0.87 and 1.80 MeV in NaI(Tl) gamma-ray spectrum. Anisotropy measurements for the 885-848, 1073-848 and 1138-885 keV cascades were carried out, and the possible spin sequences were given for them. A decay scheme is proposed with energy levels (and spins) in ^{134}Xe at 848(2+), 1615(2+), 1733(4+), 1921(3,2), 2138, 2274, 2355, 2410, 2591, 2658, 2870(4,5), 3224, and 3379 keV. The levels, which are populated by strong beta groups, are also confirmed by a summing spectrum measurement. The half-life of ^{134}I was obtained to be (52.5 ± 0.1) minutes.

RADIOACTIVITY ^{134}I (from fission) ; measured $T_{\frac{1}{2}}$, E_γ , I_γ , $\gamma\gamma$-coin, $\gamma\gamma(\theta = 90^o, 180^o)$; ^{134}Xe deduced level, J, π . Ge(Li) and NaI(Tl) detectors.

I-D-2. An Empirical Correlation Formula of Spontaneous Fission Half-Lives

E. Takekoshi

A paper on this subject has been submitted to Nuclear Data (A) with an abstract as follows :

A simple empirical correlation formula has been proposed separately for the spontaneous fission half-life data on the nuclides in the range from Pu to Fm and the nuclides in the wider range from Th to element-104, based on Swiatecki's correlation formula. The forms of correlation function proposed in the present work are in the relation of $\log_{10}T(\text{years}) = c_1 X + c_2(1 - X)\ \delta M + c_3 + \Delta$ for the nuclides in the range from Pu to Fm, and in the relation of $\log_{10}T(\text{years}) = c_1(1 - X)^3 + c_2(1 - X)\ \delta M + c_3 + \Delta$ for the nuclides in the wider range from Th to element-104. The X value is defined as the fissility parameter in each mass formula, and the δM value in MeV as the mass deviation of the experimental mass from the liquid drop mass in the mass formula. These values are calculated by using the first set and the second set of Myers & Swiatecki mass formulas and also by using Seeger & Perisho mass law. In the wider range, the results in use of a semi-empirical correlation function with the theoretical barrier are also examined. Among these correlation formulas, the correlation formula with the smallest weighted variance was obtained to be $\log_{10}T(\text{years}) = 2821.608(1 - X)^3 - 25.285(1 - X)\ \delta M - 18.949 + \Delta$ (3.725 for odd-A nuclides and 3.363 for odd-odd nuclides), in use of the second set of Myers & Swiatecki mass formula. By using this formula, spontaneous fission half-lives were examined for even-even nuclides of Z = 102, 104, 106 and 108, and compared with the results obtained by Viola & Wilkins.

E. Japanese Nuclear Data Committee

I-E-1. A Review of Carbon Total Neutron Cross Section up to 2 MeV

K. Nishimura, S. Igarasi, S. Tanaka and T. Fuketa

A full paper on this subject, which was outlined in the EANDC (J) 10 "L p. 19, has been submitted to Newsletter of the ENEA Neutron Data Compilation Centre.

I-E-2. Inelastic Scattering of Neutrons by U-238

S. Igarasi, T. Murata* and H. Nakamura**

Though many evaluation works[1)] on the inelastic scattering of ^{238}U have been made, there are some discrepancies among the results of these works.

Review and evaluation of total and partial excitation cross sections of ^{238}U are carried out to obtain self-consistent values of these cross sections in the range of neutron energy from threshold to 15 MeV. Calculations are performed by using optical model, Hauser-Feshbach method and evaporation model. To look for a systematic parameter set of the optical potential, investigations are made about the excitation cross sections for low-lying levels below 1 MeV. In the high energy region above 1 MeV, inverse cross sections obtained by the parameter set are used in the evaporation model. It is necessary to get a smooth curve by connecting

---

* Nippon Atomic Industry Group Co. Ltd.

** Fuji Electric Co. Ltd.

cross sections in the low and the high energy regions.

Reference :

1) J.J. Schmidt ; Neutron Cross Sections for Fast Reactor Materials, KFK 120 (1966).

I-E-3. Evaluation of Neutron Capture Cross Sections of Cr, Fe, Ni and Mo in the keV and MeV region

K. Nishimura, T. Asami, S. Igarasi, M. Hachya,* and H. Nakamura**

A working group on compilation of neutron capture cross section has been started by asking the numerical data in SCISRS from CCDN and surveying published reports. The component elements of stainless steel, i.e. Cr, Fe, Ni, and Mo as well as their separate isotopes, are selected for the object. A preliminary calculation of neutron capture cross sections for the above natural elements has been carried out by making use of RACY programme.

* Mitsui Shipbuilding & Engineering Co., Ltd.

** Fuji Electric Co., Ltd.

I-E-4. Calculations of Neutron Transmission Coefficients (A = 20 to 79)

S. Igarasi

Tables[1] of the neutron transmission coefficients are presented for mass number region A = 20 $\sim$ 79, by using the computer code ELIESE-2 [2] Energy range and energy intervals used are

$$E = 0.2 \text{ to } 9.0 \text{ MeV with } \Delta E = 0.2 \text{ MeV},$$

and

$$E = 9.0 \text{ to } 24.0 \text{ MeV with } \Delta E = 1.0 \text{ MeV}.$$

Parameters of the optical potential used are

$$\begin{aligned} V_{cR} &= 48 - 0.29\,E && \text{(MeV)},\\ W_s &= 9 \text{ (MeV)} && \text{(Gaussian)},\\ V_{so} &= 10 - 0.15\,E && \text{(MeV)},\\ r_o &= r_s = 1.25 && \text{(fermis)},\\ a_o &= 0.65 && \text{(fermis)}, \end{aligned}$$

and

$$b = 0.98 \qquad \text{(fermis)}.$$

References :

1) S. Igarasi, Neutron Transmission Coefficients (A = 20 to 79) JAERI-memo 3368 (1969).

2) S. Igarasi, Program ELIESE-2, JAERI-1169 (1968).

II. Kyoto University Research Reactor Institute

II-1. Measurement of Average Cross Section for Some Threshold Reactions to the Fission-Type Reactor Spectrum

I. Kimura, K. Kobayashi and T. Shibata

A paper on this subject will be submitted to Journal of Nuclear Science and Technology soon.

The energy spectrum of fast neutrons in Kyoto University Reactor, KUR, which is a light-water-moderated, 90 %-enriched-fueled research reactor of 5,000 KW, was measured with threshold detectors,[1)2)] with a ^{6}Li sandwich counter[3)] and with nuclear plates. The result shows that the spectrum is close to the fission neutron spectrum, as in Fig. 1 and Fig. 2.

Accodingly, the average cross sections for some threshold reactions to this fission-type reactor spectrum become measurable in the core of KUR. The average cross sections for nine threshold reactions, $^{46}Ti(n,p)^{46}Sc$, $^{47}Ti(n,p)^{47}Sc$, $^{48}Ti(n,p)^{48}Sc$, $^{28}Si(n,p)^{28}Al$, $^{29}Si(n,p)^{29}Al$, $^{30}Si(n,\alpha)^{27}Mg$, $^{64}Zn(n,p)^{64}Cu$, $^{204}Pb(n,n')^{204m}Pb$ and $^{204}Pb(n,2n)^{203}Pb$, have been obtained.

A Ge(Li) counter was mainly used to measure the relative value of induced activities. For the absolute measurement, several standard gamma sources calibrated by IAEA were used. As fast neutron flux monitors, $^{58}Ni(n,p)^{58}Co$, $^{24}Mg(n,p)^{24}Na$, and $^{27}Al(n,\alpha)^{24}Na$ were adopted and the fluxes measured with these monitor foils agreed within 2 %. In addition to this error, the statistical error and the systematic error that was estimated to be about 5 % were taken into account. The final results are tabulated in from Table 1 to Table 9.

References :

1) I. Kimura, K. Kobayashi and T. Shibata, Ann. Reports, Research Reactor Institute, Kyoto University, 1 (1967/1968) 95.

2) K. Kanda, T. Nanjo, K. Kobayashi, Y. Nakagome and I. Kimura, Ann. Reports, Research Reactor Institute, Kyoto University, 2 (1969) 18.

3) I. Kimura, S. Hayashi, K. Kobayashi, S. Ishihara and T. Shibata, "The Measurement of Fast Neutron Spectrum with ^{6}Li and ^{3}He Sandwich Counters" KURRI-TR to be published.

4) J. Comera, Interner CEA-Report, DPE-SPE, Note E87 (1963).

5) R.W. Durham, et al., AECL-1434 (1962).

6) J.W. Boldeman, J. Nucl. Energy A/B 18 (1964) 417.

7) W. Köhler, Nukleonik 8 (1966) 9.

8) A.M. Bresesti, et al., Nucl. Sci. Eng. 29 (1967) 7.

9) S. Niese, et al., Kernenergie 6 (1963) 37.

10) C.H. Hogg, et al., ASTM Special Tech. Publ. No. 341 (1963).

11) J.C. Roy and J.J. Hawton, AECL-1181 (1960).

12) C.E. Mellish, AERE-R/325 1 (1960).

13) R. Beaugé, "Sections efficases pour les détecteurs de neutrons par activation recommandées par le groupe de dosimetrie d'Euratom" (1963).

14) W. Köhler and K. Knopf, Nukleonik 10 (1967) 181.

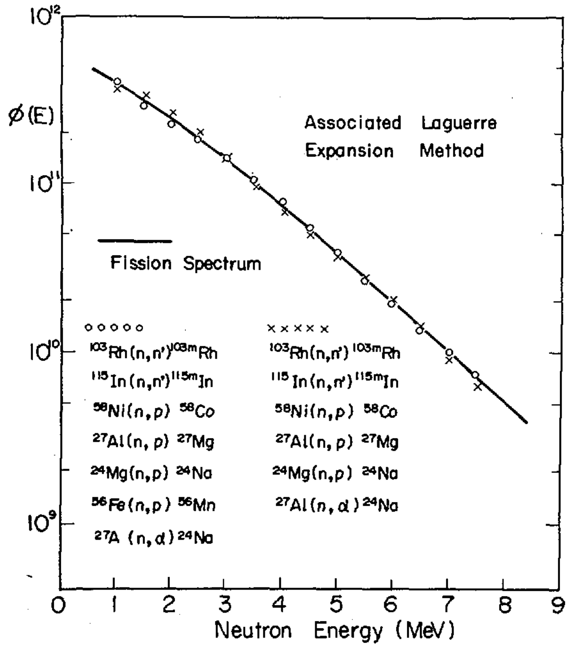

Fig. 1 Fast Neutron Spectrum in KUR Core obtained with Threshold Detectors.

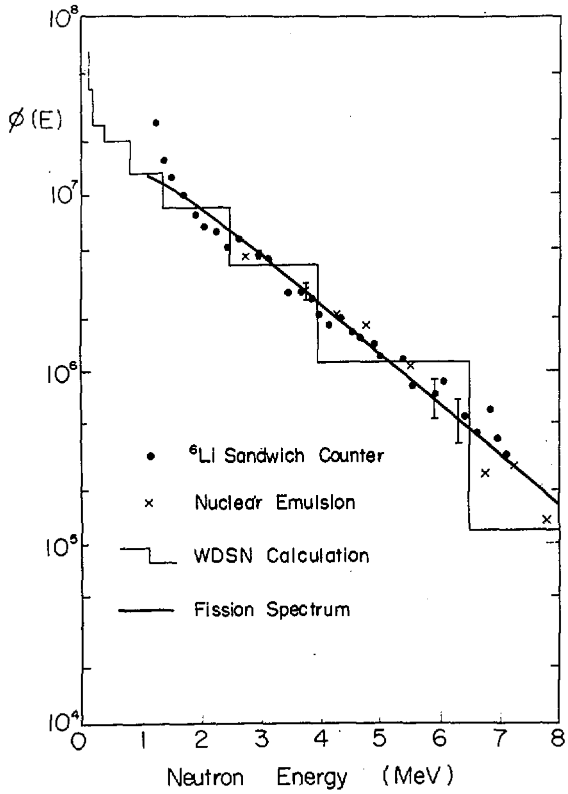

Fig. 2 Fast Neutron Spectrum in KUR Core obtained with ^{6}Li Sandwich Counter, with Nuclear Plates and WDSN Theoretical Calculation.

Table 1. Data of $^{46}Ti(n,p)^{46}Sc$ Reaction Cross Section Averaged over Fission Spectrum

Cross Section (mb)	Reference
11.2 ± 0.6	Present Data
11.1	Comera (4)
10	Durham (5)
12.8 ± 0.6	Boldeman (6)
12.6 ± 0.4	Köhler (7)
10.2 ± 0.4	Bresesti (8)

Table 2. Data of $^{47}Ti(n,p)^{47}Sc$ Reaction Cross Section Averaged over Fission Spectrum

Cross Section (mb)	Reference
19.2 ± 1.2	Present Data
18	Durham (5)
18 ± 3	Niese (9)
15 ± 0.6	Hogg (10)
22 ± 1.5	Boldeman (6)
13.2 ± 1.0	Köhler (7)

Table 3. Data of $^{48}Ti(n,p)^{48}Sc$ Reaction Cross Section Averaged over Fission Spectrum

Cross Section (mb)	Reference
0.29 ± 0.02	Present Data
0.53	Durham (5)
0.44 ± 0.08	Niese (9)
0.25 ± 0.01	Hogg (10)
0.21 ± 0.016	Boldeman (6)
3.3 ± 0.2	Köhler (7)

Table 4. Data of $^{28}Si(n,p)^{28}Al$ Reaction Cross Section Averaged over Fission Spectrum

Cross Section (mb)	Reference
4.9 ± 0.3	Present Data
4.0	Roy (11)

Table 5. Data of $^{29}Si(n,p)^{29}Al$ Reaction Cross Section Averaged over Fission Spectrum

Cross Section (mb)	Reference
3.0 ± 0.2	Present Data
2.7	Roy (11)

Table 6. Data of $^{30}Si(n,\alpha)^{27}Mg$ Reaction Cross Section Averaged over Fission Spectrum

Cross Section (mb)	Reference
0.13 ± 0.02	Present Data
0.15 ± 0.02	Niese (9)

Table 7. Data of $^{64}Zn(n,p)^{64}Cu$ Reaction Cross Section Averaged over Fission Spectrum

Cross Section (mb)	Reference
36 ± 3	Present Data
44	Mellish (12)
39	Roy (11)
31	Durham (5)
33	Beaugé (13)
27 ± 1.6	Boldeman (6)

Table 8. Data of $^{204}Pb(n,n')^{204m}Pb$ Reaction Cross Section Averaged over Fission Spectrum

Cross Section (mb)	Referance
19 ± 2	Present Data
22	Durham (5)
15.3 ± 0.7	Köhler (14)

Table 9. Data of $^{204}Pb(n,2n)^{203}Pb$ Reaction Cross Section Averaged over Fission Spectrum

Cross Section (mb)	Reference
1.9 ± 0.2	Present Data
3.3	Roy (11)
5.0	Durham (5)

III. Kyushu University

Department of Nuclear Engineering

III-1. (n,n) and (n,n') Reactions of B and B^{10} Induced by 14-MeV Neutrons

M. Hyakutake, M. Matoba, H. Tawara, Y. Wakuta, A. Katase and M. Sonoda

Elastic and inelastic scattering cross sections of 14.1-MeV neutrons have been measured for enriched B^{10} and natural boron by associated-particle time-of-flight technique. Scattered neutrons were not resolved completely and were measured as some groups. Differential cross sections at laboratory angles between 10° and 160° were obtained for these groups of neutrons which correspond to the following Q-values respectively.

B^{10} :	n_0	Q = 0, 0.717 MeV
	n_1	Q = 1.74, 2.15 MeV
	n_2	Q = 3.59 MeV
	n_3	Q = 4.77, 5.11, 5.17, 5.18 MeV
	n_4	Q = 5.92, 6.03, 6.13 MeV
	n_5	Q = 6.57, 6.88, 7.00 MeV
B^{11} :	n_0	Q = 0
	n_1	Q = 2.12 MeV
	n_2	Q = 4.44 MeV
	n_3	Q = 5.02 MeV
	n_4	Q = 6.74, 6.79 MeV

The differential elastic scattering cross sections are shown in Figs. 1 and 2 in comparison with those found by Alder et al.[1] Corrections for multiple scattering, flux attenuation and angular resolution are now in progress. Analyses of the data are to be carried out by optical model and DWBA method.

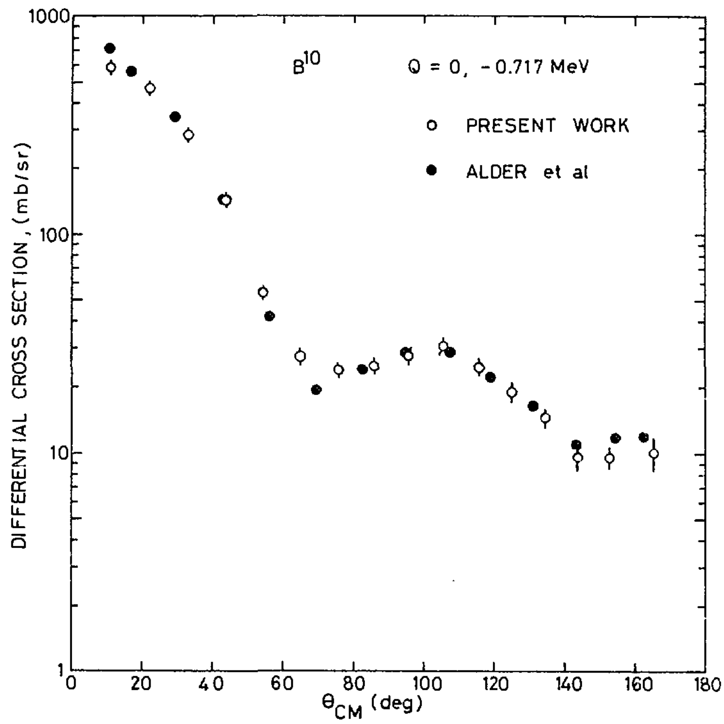

1000
100
10
1
DIFFERENTIAL CROSS SECTION, (mb/sr)
B^{10}
Q = 0, -0.717 MeV
PRESENT WORK
ALDER et al
0
20
40
60
80
100
120
140
160
180
θ_{CM} (deg)

Fig. 1

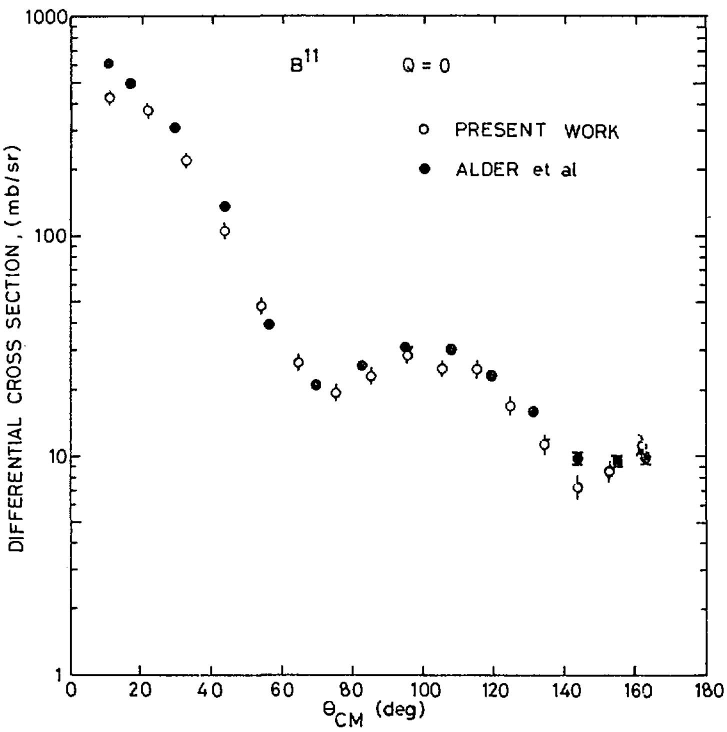

1000
100
10
1
DIFFERENTIAL CROSS SECTION, (mb/sr)
B^{11}
Q = 0
PRESENT WORK
ALDER et al
0
20
40
60
80
100
120
140
160
180
θ_{CM} (deg)

Fig. 2

Reference :

1) J.C. Alder, B. Vaucher and C. Joseph, Helv. Phys. Acta, 41 (1968) 433.

III-2. (n,n) and (n,n') Reactions of Be^9 Induced by 14-MeV Neutrons

M. Hyakutake, M. Matoba, H. Tawara, Y. Kanda, A. Katase and M. Sonoda

Elastic and inelastic scattering cross sections of 14.1 MeV neutrons have been measured for Be^9 by associated-particle time-of-flight technique at laboratory angles between 10° and 165°. Over-all time resolution (FWHM) was about 1.8 nsec at a detector bias corresponding to 3.5 MeV neutron.

Neutrons inelastically scattered from 2.43 MeV state of Be^9 were well resolved from elastically scattered neutrons.

The differential elastic and inelastic scattering cross sections are shown in Figs. 1 and 2 in comparison with those found by Nakada et al.[1)] and Anderson et al.[2)] However, in our data corrections for multiple scattering, flux attenuation and anguler resolution are not yet made. These corrections and analyses by optical model and DWBA method are now in progress.

References :

1) M.P. Nakada, J.D. Anderson, C.C. Gardner and C. Wong, Phys. Rev. 110 (1958) 1439.

2) J.D. Anderson, C.C. Gardner, J.W. McClure, M.P. Nakada, Phys. Rev. 111 (1958) 572.

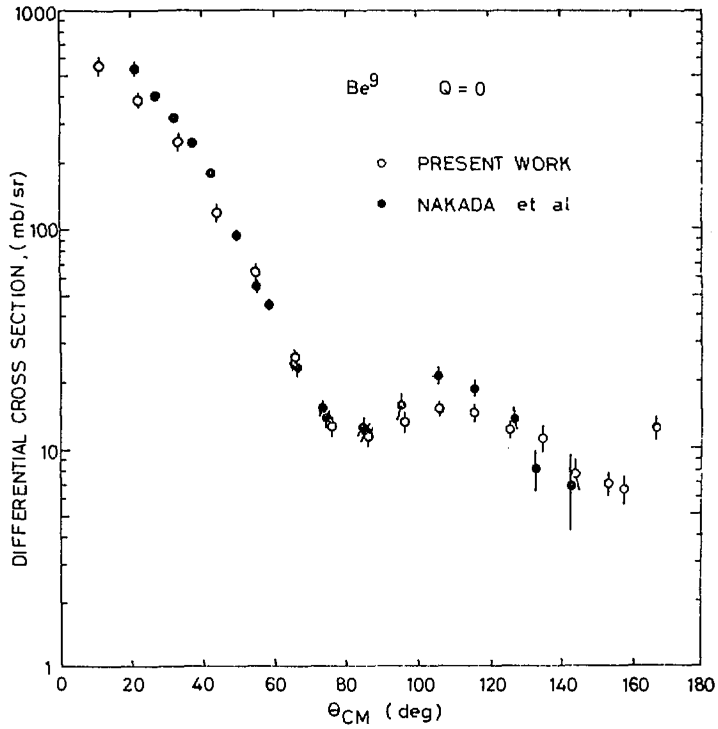
Be^9 Q = 0
PRESENT WORK
NAKADA et al
DIFFERENTIAL CROSS SECTION, (mb/sr)
1000
100
10
1
0
20
40
60
80
100
120
140
160
180
θ_{CM} (deg)

Fig. 1

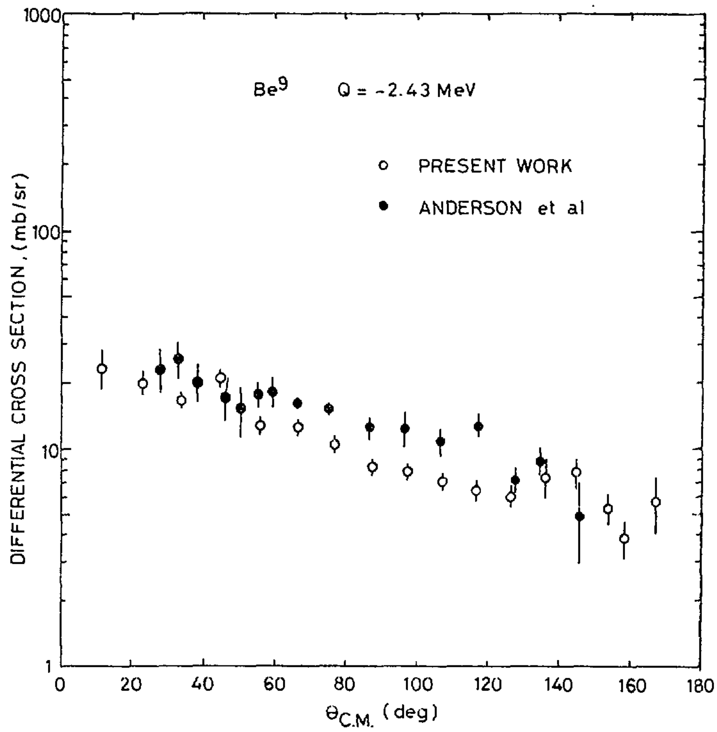
Be^9 Q = -2.43 MeV
PRESENT WORK
ANDERSON et al
DIFFERENTIAL CROSS SECTION, (mb/sr)
1000
100
10
1
0
20
40
60
80
100
120
140
160
180
$\theta_{C.M.}$ (deg)

Fig. 2

III-3. Improvements of Fast Neutron Time-of-Flight Spectrometer

M. Matoba, H. Tawara, M. Hyakutake, Y. Wakuta, A. Katase
and M. Sonoda

To study the inelastic scattering of neutrons, the cross sections of which are small ($d\sigma/d\Omega \lesssim 1$ mb/sr.), the following two improvements have been carried out.

(1) Reduction of background

With the time-of-flight system[1)] used for the study of the neutron scattering the attenuation of 14 MeV neutrons through iron blocks was accurately measured. The information on the design of a shadow bar and the shield was obtained.

Two types of the shield of the neutron detector were constructed. One of them is iron blocks 10 cm thick and lead ones 10 cm thick, the other one is paraffin blocks (mixed with boric acid) 30 cm thick and lead ones 10 cm thick. The background was reduced by one order compared to the one in the case of the bare neutron detector for both types of the shield.

(2) Improvement of time resolution

A new and simple method was designed to compensate electronically the rise-time effect of the neutron detector on the time resolution. Obtained time resolution was less than 1.2 nsec. This resolution is nearly equal to the one due to only the geometry of our time-of-flight system.

After these improvements, measurements of (n,n') reaction of nitrogen are in progress.

Reference :

1) M. Sonoda et al. EANDC (J) 10 "L" (1968) p. 25.

III-4. Photo-Fission Cross Sections of the Medium Mass Nuclei

A. Katase, M. Matoba, Y. Kanda, M. Chijiya, M. Sonoda,
Y. Wakuta, H. Tawara and M. Hyakutake

The photo-fission cross sections of Ho, Sm, Te, Sb, Sn, In, Ag, Ge, Cu and Au were measured for the energies of 1000, 600, 450 and 250 MeV.

In one experiment, two detector foils of polycarbonate, onto one of which the pure metal was evaporated, were put together to form a sandwitch by grewing at one end of the foils. A stack of such sandwitches was irradiated by the collimated photon beam of about 1 cm in diameter. After irradiation the metals were solved with HNO_3 solution. The detector foils were subsequently etched in NaOH solution. The fission tracks were observed with an optical microscope. The track length of each fission fragment was measured for the paired tracks to investigate the range-ratio distribution of the fragments.

In the other experiment, a polycarbonate detector foil was pressed on a target film evaporated on a polycarbonate backing. The detector foil was exchanged for each irradiation, the same target being used throughout the experiments, in order to investigate the variations of the fission cross section with the photon energy and the fissionability with the atomic number of target material.

The scanning and analysis are now in progress.

IV. Osaka University

Department of Nuclear Engineering

IV-1. Lattice Vibrational and Rotational Frequency Distribution in Bezene Crystal and the Comparison with Neutron Scattering Data

T. Sekiya, K. Sakamoto* and Y. Watari**

To analyse the neutron scattering data for solid and liquid benzene[1,2) calculation code has been made under the support of Japanese Nuclear Data Committee.

The principle is based on FG matrix method generalized to the case of the periodic structure. The results show good agreement with the fine structure of solid benzene scattering cross section observed by Zemlianov.[3) At the same time we find the reason of the discrepancy between scattering peaks of Tarinǎ's data and the theoretical results evaluated by Shimanouchi and Harada for $q = 0$ case.[4)

References :

1) V. Tarinǎ, J. Chem. Phys. 46 (1967) 3273.

2) M.G. Zemlianov, N.A. Tschernoplekov ; Atomnaya Energia 14 (1963) 257.

3) T. Sekiya, K. Sakamoto and Y. Watari ; JAERI-memo (to be published).

4) I. Harada and T. Shimanouchi ; J. Chem. Phys. 44 (1966) 2016.

---

* Okayama Colleage of Science.

** Hitachi Comp., Ltd.

V. Radiation Center of Osaka Prefecture

V-1. Scattering Cross-Sections of 14-MeV Neutrons

T. Azuma and Y. Sato

The scattering cross-sections of 14-MeV neutrons were measured for the elements of ^{12}C, ^{16}O, ^{27}Al and ^{208}Pb. The energy spectra of scattered neutrons were observed by α n associated particle time-of-flight method, in which the deuteron beams of 0.4 MeV, 30 μ A, from the Van de Graaff bombarded the tritium target. The α-detector was NE102A-56AVP, the neutrons NE213-6810A, and Eldorado Model 300 TPC system. The flight path was 160 cm and the accumulation time was about 6 hours (1.2×10^9 α-counts).

The characteristics of the detecting system are the following ; 1) the snap-off diode SV14B is used, 2) the energy gate circuits are applied to the start and stop inputs of the TPC, 3) the resolving time of the system is 1.5 ns, 4) the shield thickness to the direct 14-MeV neutrons is 50 cm Fe, and 5) the neutron detection efficiency is 2.5 percents for the energy gate of 7 MeV, which was estimated with the values of 150 and 40 mb at 35 degrees for ^{12}C, 4.43-MeV level.

The elastic scattering cross-section is calculated using the equation,

$$\sigma(\theta) = \sum_{\ell=0}^{\infty} \frac{2\ell+1}{4\pi} \cdot B_\ell \cdot P_\ell \ (\cos\theta)$$

where the values of B_ℓ are taken from the table at $\overline{R} = 1.25\ A^{1/3} + 0.5$.

The inelastic scattering cross-sections are calculated using the equations of Hauser and Feshbach,[1] for s-neutrons :

$$A(\ell j \,|\, \ell' j \,|\, \theta) = \sum_{n=0}^{\ell'} \cdot S_n\ (\ell j \,|\, J) \cdot F_n\ (J \,|\, \ell' j' \,|\, \theta),$$

where J is the compound nucleus spin, the neutron orbital angular momentum $\ell \rightarrow \ell'$, and the channel spin $j \rightarrow j'$.

The measured angles are 25, 35, 45 and 55 degrees. The values at 35 degrees are listed in the table. The pulse shape discrimination is now tested.

Elements	level MeV	$\sigma(\theta)$ mb at 35°
Carbon	4.43	40
H_2O	6.05	5 ± 2.0
Aluminum	4.05	4 ± 1.5
Lead	4.1	8 ± 2.5

Reference :

1) W. Hauser and H. Feshbach, Phys. Rev. 87 (1952) 366.

VI. Tokyo Institute of Technology

VI-1. Measurements of Neutron Inelastic Scattering Cross Sections of Deuteron $\sigma(E_p, E_{n'}, \theta_{n'})$ at an Incident Neutron Energy of 14.5 MeV

E. Arai, M. Ito* and T. Yamauchi

The break-up reactions of deuterons by fast neutrons has been studied because of its nuclear physical interest as it is a typical three particle reaction and also from the standpoint of nuclear data accumulation for nuclear reactors.

To obtain a complete information on the reaction mechanism, it is desired to determine five independent variables.

In many works, however, only three variables of the five have been determined, namely $\sigma(E_{n'}, \theta_{n'})$[1] or $\sigma(E_p, \theta_p)$[2] was observed.

These results and the theoretical predictions suggest that we can observe effects of the n-p residual interaction at $E_{n'} \cong 5$ MeV and $E_p \cong 5$ MeV and those of the n-n residual interaction at $E_{n'} \cong E_{n''} \cong 0.3$ MeV and $E_p \cong 12$ MeV.

Main purpose of this report is to investigate experimentally effects of these final state interactions in the neutron cross sections of deuterons $\sigma(E_p, E_{n'}, \theta_{n'})$. Here four variables of the reaction kinematics were determined. 14.5 MeV neutrons were generated by means of the reaction of T $(d,n)\alpha$, where the deuterons were accelerated by the cascade type machine with a voltage of 350 kV.

An application of the associated α particle method enabled us to

* Denden Kosha Tsushin Kenkyusho

determine the energy distribution of inelastically scattered neutrons by means of time of flight method. A liquid scintillator of NE230 was set at the center of a goniometer and served as the scattering sample. Its main constituent is C_6D_6 and its active volume has a dimension of 50 mmϕ $\times$ 30 mm which is large enough to cover the neutron cone at a distance of 23 cm from the tritium target. A 56 AVP was coupled to the scintillator and gave the pulse height signal and the timing signal of neutron scattering. The former signal was fed to Y-axis with 5 bits of the 4096 channel pulse height analyser of Van de Graaff Lab. of the Tokyo Kogyo Daigaku. The timing signal and that of the α-detector were sent to a fast coincidence unit, whose coincidence signal stopped the time to amplitude converter.

A plastic scintillator with a dia. of 175 mmϕ and a thickness of 25 mm detected the scattered neutrons and generated start signals for the TAC. The neutron flight path measured 185 cm and the overall time resolution of the system was 2.0 nsec. The output of the TAC was fed to X-input with 7 bits of the 4096 channel analyser.

The detection efficiency of the neutron counter, which was necessary to calculate the cross sections from the measurements, was determined by replacing the scattering sample with normal benzene scintillator, NE 231. The elastic peak observed in the 32 $\times$ 128 channel two dimensional display was utilized to calibrate Ep-axis of the analyzer.

The Fig. shows one of the measurements where incident neutron energy was 14.5 MeV, $\theta_{n'}$ (lab) = 20°. There are three distributions like mountains. From left to right, one relatively broad distribution shows the inelastic neutrons, the central sharp peaks are the elastic neutrons and finally the low straight distribution is gamma-rays caused by the inelastic scattering on carbon atoms and atoms of constructing materials of the scatterer.

References :

1) M. Brüllmann, H. Jung, D. Meiner & P. Marmier, Nucl. Phys. 25B (1967) 269.

2) S. Shirato & N. Koori, Nuclear Physics A120 (1968) 387.

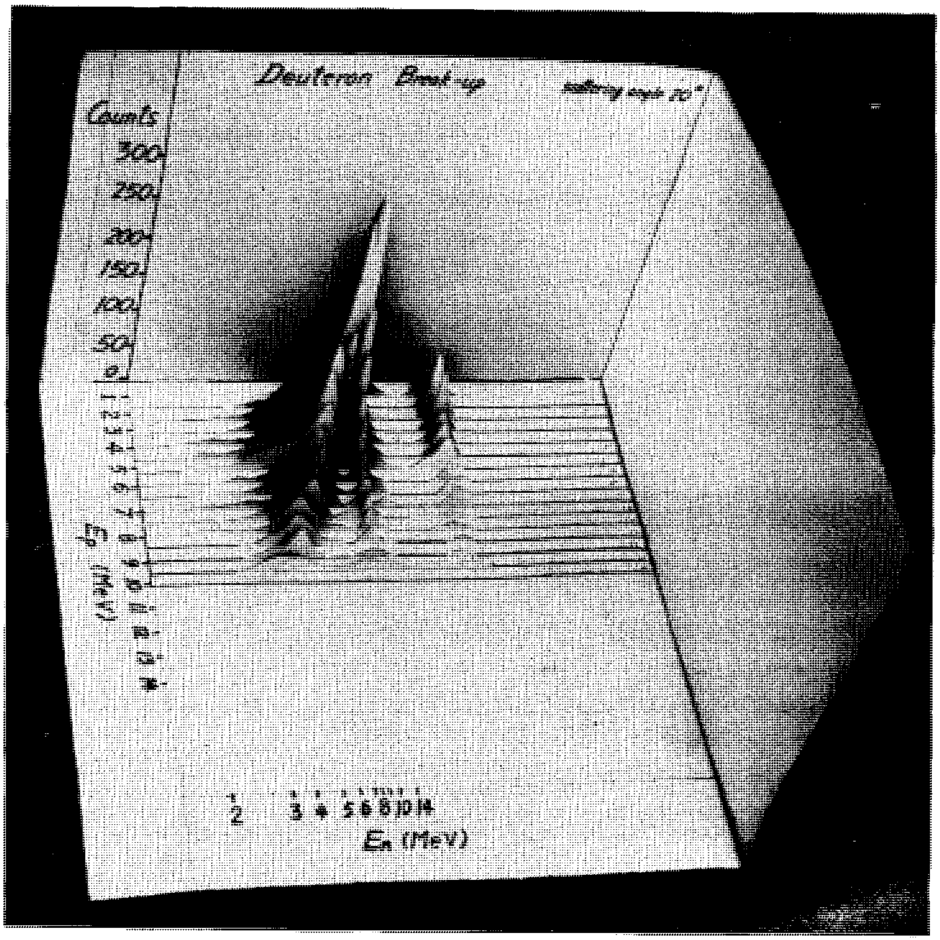

VII. University of Tokyo
Institute for Solid State Physics

VII-1. Nuclear Spin-Spin Effect in the Total Cross Section for 1 MeV Polarized Neutrons on Polarized ^{59}Co Nuclei

K. Nagamine,* A. Uchida, A. Mikuni, T. Suzuki, M. Imaizumi,
Shinroku Kobayashi and Shinsaku Kobayashi

A paper on this subject was published in the Technical Report of the Institute for Solid State Physics, the University of Tokyo, Ser. A, No. 371, July 1969.

The abstract follows :

Measurements of the spin-spin effect, $\sigma_{ss} = (\sigma\uparrow\uparrow - \sigma\uparrow\downarrow)/2P_n \cdot P_I$, in the total cross section for polarized neutrons on polarized ^{59}Co are reported at the neutron energies of 1.1 and 1.4 MeV. The degree of target polarization from 0.47 to 0.30 was obtained for a polycrystalline metal of $Co_{0.90} - Fe_{0.10}$ alloy at demagnetization temperatures from 0.030 to 0.048 °K. The results of σ_{ss} are -190 ± 140 mb at 1.1 MeV and -150 ± 180 mb at 1.4 MeV. If σ_{ss} is assumed to arise from a spin-spin term in the optical potential of the form $-V_{ss} f(r) \vec{\sigma} \cdot \vec{I}$, the strength of the potential is 200 keV $< V_{ss} <$ 800 keV combining with the published data for σ_{ss} at 7.90 MeV and assuming f(r) as a microscopic form factor. A weak and attractive nature of the spin-spin interaction is qualitatively explained by a microscopic model.

* Present Address : Department of Applied Physics, Faculty of Engineering, University of Tokyo.

VII-2. The Spin-Spin Interaction of 7.90 MeV Polarized Neutrons with Polarized ^{59}Co Nuclei

Shinsaku Kobayashi, K. Nagamine, A. Uchida, K. Katori, M. Imaizumi and A. Mikuni

A paper of this title was published in Prog. Theor. Phys. 40 (1968) 1451.